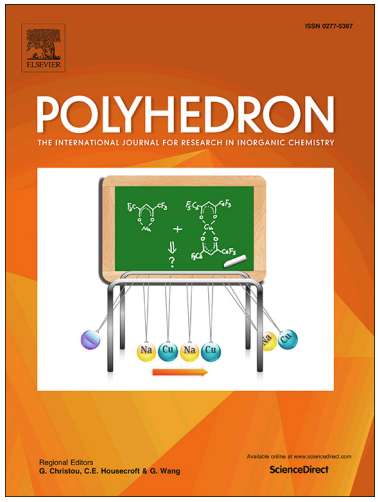

DNA interaction and anticancer properties of new peripheral phthalocyanines carrying tosylated 4-morpholinoaniline units

Halise Yalazan, Burak Barut, Beytullah Ertem, Can Özgür Yalç ın, Yasemin Ünver, Arzu Özel, İpek Ömeroğlu, Mahmut Durmuş, Halit Kantekin

PII: S0277-5387(19)30764-8
DOI: https://doi.org/10.1016/j.poly.2019.114319
Reference: POLY 114319

To appear in: *Polyhedron*

Received Date: 23 November 2019
Accepted Date: 18 December 2019

Please cite this article as: H. Yalazan, B. Barut, B. Ertem, C.O. Yalç ın, Y. Ünver, A. Özel, I. Ömeroğlu, M. Durmuş, H. Kantekin, DNA interaction and anticancer properties of new peripheral phthalocyanines carrying tosylated 4-morpholinoaniline units, *Polyhedron* (2019), doi: https://doi.org/10.1016/j.poly.2019.114319

DNA interaction and anticancer properties of new peripheral phthalocyanines carrying tosylated 4-morpholinoaniline units

Halise Yalazan[1], Burak Barut[2], Beytullah Ertem[3,*], Can Özgür Yalçın[4,5] Yasemin Ünver[1], Arzu Özel[2,5], İpek Ömeroğlu[6], Mahmut Durmuş[6], Halit Kantekin[1]

[1]Department of Chemistry, Karadeniz Technical University, 61080, Trabzon, Turkey

[2]Faculty of Pharmacy, Department of Biochemistry, Karadeniz Technical University, 61080, Trabzon, Turkey

[3]Vocational School of Health Services, Karadeniz Technical University, 61080, Trabzon, Turkey

[4]Faculty of Pharmacy, Department of Toxicology, Karadeniz Technical University, 61080, Trabzon, Turkey

[5]Drug and Pharmaceutical Technology Application and Research Center, Karadeniz Technical University, 61080, Trabzon, Turkey

[6]Department of Chemistry, Gebze Technical University, Gebze, 41400, Kocaeli, Turkey

*Author for correspondence: Beytullah Ertem

Karadeniz Technical University, Vocational School of Health Services, 61080, Trabzon, Turkey

Tel.: +90 462 377 57 03, Fax: +90 462 325 29 33, e-mail: bertem@ktu.edu.tr

ABSTRACT

In this paper, tosylated 4-morpholinoaniline units fused peripherally tetra-substituted free-base **(5)**, copper(II) **(6)**, zinc(II) **(7)**, cobalt(II) **(8)** and magnesium(II) **(9)** phthalocyanines (Scheme) were reported and these new phthalocyanine conjugates were characterized through Fourier Transform–Infrared (FT–IR) with ATR sampling accessory, Mass Spectra Analysis [Matrix Assisted Laser Desorption/Ionization–Time of Flight–Mass Spectral (MALDI–TOF–MS)] and Ultraviolet-visible (UV–vis) (for all new phthalocyanines), elemental analysis, as well as ^{1}H and ^{13}C NMR spectroscopic techniques [for the compounds **(2)**, **(4)**, **(5)**, **(7)** and **(9)**]. The potential utilization of the new peripheral phthalocyanine compounds (**7** to **9**) as the new pharmaceutical agents in PDT applications (in oncology and molecular biology) were determined in aspects of pBR322 plasmid DNA cleavage on agarose gel electrophoresis. The results showed that compound **(7)** cleaved pBR322 plasmid DNA with irradiation. Compound **(7)** displayed hypochromism without any shift on the addition of increasing concentrations of ct-DNA and K_b of compound **(7)** was calculated as 2.45 ± (0.20) × 10^4 M^{-1}. In photochemical studies, the Φ_Δ value of compound **(7)** was determined as 0.11. The cytotoxic/phototoxic properties of compound **(7)** which had the best photocleavage effects among tested compounds were investigated using MTT assay toward human colorectal (HCT-116) and cervical (HeLa) cancer cells. The cell viabilities of compound **(7)** were found to be 73 ± 1.6% (HCT-116) and 65 ± 5.5% (HeLa) at 100 μM with irradiation.

Keywords: DNA interaction; Anticancer studies; Phototoxicity; Cytotoxicity; Zinc(II) phthalocyanine; 4-Morpholinoaniline.

1. Introduction

Being a member of aromatic heterocyclic macrocyclic compounds, phthalocyanines (Pcs) consist of four pyrrole ring where 18 π-electron cloud is delocalized over carbon and nitrogen atoms with a coplanar configuration [1,2]. Since their accidental discovery during the production of phthalimide from phthalic anhydride, phthalocyanines have been of great significance because of their unique intense color, high inertness, thermal stability, and low solubility [3–5]. As such, phthalocyanines have been used extensively as a coloring agent in the industrial productions of paint, printing, and textile. Depending on the developments in the chemistry of Pcs, they have been discovered to own exciting and tunable electronic, photochemical, photophysical, optical, self-assembling and catalytic features in various disciplines [4,5]. To put it another way, above mentioned properties made phthalocyanines to broaden their utilization from industrial dyestuffs and pigments to various medicinal, biomedical, chemical, and high-technological applications serving as photosensitizing agents for photodynamic therapy [6,7], fluorescent probes for bioimaging and bioanalysis [8–10], photovoltaics [11,12], sensors [12–14], molecular electronics [15], electrocatalysis [16], electrochromic displays [17], electrophotography [18], dye-sensitized solar cells [19], and as well as nonlinear optical (NLO) materials [20]. To that end, there has been a growing interest and effort to investigate the synthesis, features, and applications of this aromatic heterocycles over the last few decades.

The nitrogen-containing heterocycles such as morpholine and its varied derivatives have attracted exceptional attention owing to their valuable antimicrobial [21,22], anti-inflammatory [23–25], central nervous system [26–29], therapeutic [30], anticancer (i.e., mammalian target of rapamycin, non-small cell lung cancer, human colorectal adenocarcinoma, prostate cancer, metastatic human breast cancer and gastric cancer) [31,32], antioxidant, pesticide and bactericide activities [33,34] during the past few decades. According to The World Drug Index, nowadays, morpholine based compounds have been made use of over 100 drugs (i.e., Gefitinib, Linezolid, and Aprepitant) [35–37] which contain morpholine ring system as a scaffold, a side-chain or a component of the fused-ring systems [38]. Other than its medicinal and pharmaceutical applications, morpholine compounds have been of considerable significance and used in a wide range of industrial applications such as in textile industry, waxes and in the preservation of book paper, air conditioners, a chemical intermediate in catalysts, an anticorrosive agent in water

boiling systems, and photographic developers [33,34]. Due to their high potential and importance, morpholine based compounds have been of great interest and a large number of studies have been carried out including morpholine bearing phthalocyanines such as water-soluble silicon phthalocyanine derivatives with DNA/BSA binding properties [39], unsymmetrical octasubstituted zinc and cobalt phthalocyanines with electrochemical and optical properties [40], water-soluble quaternized zinc phthalocyanine with PDT and protein binding properties [41] and octasubstituted quaternized magnesium phthalocyanine with antimicrobial and anticancer activities of adenocarcinomic alveolar basal epithelial cells and human oral squamous carcinoma cells [42]. To the best of our knowledge, there is no published study that contains the investigation of anticancer properties of tetra-substituted peripheral metallophthalocyanine carrying tosylated morpholine derivative in the literature. In line with this goal, we preferred choosing a different type of morpholine derivative, 4-methyl-*N*-(4-morpholinophenyl)benzenesulfonamide, fused to the phthalocyanine scaffold to investigate the anticancer properties toward human colorectal (HCT-116) and cervical (HeLa) cancer cells.

In today's modern life, cancer is among the prominent diseases that are responsible for mortality [43,44]. In combat against cancer, several applicable treatment methods exist in practice such as surgery, chemotherapy and radiation therapy as well as phytotherapy (as the complementary medicine) [45,46] have been applied currently in medicine. For the treatment of cancer, in general, a combination of surgery with the aforementioned therapeutic methods is applied. In addition to the foregoing treatments, an alternative therapeutic modality has been used to treat many kinds of cancer types. This innovative and attractive modality is called photodynamic therapy (PDT) depending upon the use of a composition of a photosensitizer (a non-toxic drug or dye), a long wavelength of red visible light (620–690 nm) [47–49] and molecular oxygen to bring about to selective destruction or damage to the localized cancer tumors [50–52]. Nowadays, PDT has been clinically approved and utilized for the treatment of some cancerous tumors (such as skin tumors, head and neck tumors, digestive system tumors, urinary system tumors, non-small cell lung cancer, and brain tumors) in medicine [53].

In light of the above-mentioned knowledge, after synthesis and structural verification, our research group has focused on the investigation of DNA cleavage and cytotoxic/phototoxic properties of morpholine bearing metallated phthalocyanine compounds to determine their suitability in the treatment of cancer diseases as the second generation photosensitizers in PDT

applications. To accomplish this goal, we synthesized the new free-base **(5)**, copper(II) **(6)**, zinc(II) **(7)**, cobalt(II) **(8)** and magnesium(II) **(9)** Pcs connected with tosylated 4-morpholinoaniline functionalities as peripheral substituents (Scheme). An agarose gel electrophoresis was employed to examine the DNA cleavage effects of the compounds (**6**–**9**). The DNA binding effect and singlet oxygen quantum yield of compound **(7)** were investigated using UV-vis spectroscopy. Besides, cytotoxic and phototoxic properties of compound **(7)** against human colorectal (HCT-116) and cervical (HeLa) cancer cells were investigated using (3-(4,5-dimethylthiazol-2-yl)-2,5-diphenyltetrazolium bromide (MTT) assay.

2. Experimental

The equipment, materials, chemicals, DNA interaction, photochemical parameters, cytotoxicity, and phototoxicity experiments were supplied as Supplementary information. The tosylated 4-morpholinoaniline derivative **(2)** [54] and 4-Nitrophthalonitrile **(3)** [55] were prepared according to the relating articles.

2.1. Synthesis

*2.1.1. Phthalonitrile derivative **(4)***

The compound **(4)** was synthesized by the modification of the procedure described in the literature [54]. Color: Light brown. Yield: 1.40 g (79.1%), m.p. 158–161 °C. Elemental analysis: Calc. (%) for $C_{25}H_{22}N_4O_3S$: C: 65.48; H: 4.84; N: 12.22; S: 6.99, Found (%) C: 64.91; H: 4.66; N: 12.00; S: 6.63. Fourier Transform Infrared: υ_{max} (cm^{-1}) = 3078–3051 (Ar C–H), 2973–2920–2887 (C–H), 2228 (C≡N), 1594 (C=C), 1509, 1492, 1451, 1361–1159 (SO_2), 1261, 1236, 1123 (CH_2–O–CH_2), 986, 908, 834, 733, 670. ^{1}H NMR (ppm, $CDCl_3$): δ = 7.65–7.43 (m, 4H, Tosylated, Ar–*H*), 7.34–7.23 (m, 3H, Ar–*H*), 7.03–6.78 (m, 4H, Ar–*H*), 3.88–3.86 (t, 4H, O–C*H*$_2$), 3.25–3.22 (t, 4H, N–C*H*$_2$), 2.46–2.45 (s, 3H, C*H*$_3$). ^{13}C NMR (ppm, $CDCl_3$): δ = 151.68, 151.66, 146.96, 145.08, 145.07, 135,87, 134.14, 134.13, 130.96, 130.95, 130.05, 130.04, 128.92, 127.77, 127.76, 126.63, 126.62, 126.13, 126.12, 116.60, 115.82–115.81–115.24–115.07 (*C*≡N), 110.24, 66.66–66.65–65.84 (O–*C*H$_2$), 48.19–48.18 (N–*C*H$_2$), 21.67–21.66 (Ar–*C*H$_3$). Mass Spectra Analysis *m/z*: 458.21 $[M]^+$.

*2.1.2. Free-base phthalocyanine (**5**)*

The new free-base phthalocyanine (**5**) was synthesized by the common synthetic procedure in which a phthalonitrile compound and a strong base (1,8-diazabicyclo[5.4.0]undec-7-ene) heated in a high boiling solvent (pentan-1-ol) under inert atmosphere as described in the literature [7]. The crude product was purified by washing it with hot ethanol to give the free-base compound **(5)**. Color: Light Green. Yield: 20.0 mg (20.0%), m.p. >300 ºC. Elemental analysis: Calc. (%) for $C_{100}H_{90}N_{16}O_{12}S_4$: C: 65.41; H: 4.94; N: 12.21; S: 6.99, Found (%) C: 64.89; H: 4.83; N: 11.79; S: 6.71. Fouirer Transform–Infrared: υ_{max} (cm^{-1}) = 3292 (N–H), 3047 (Ar C–H), 2956–2921 (C–H), 1600, 1509, 1449, 1348–1160 (SO_2), 1119 (CH_2–O–CH_2), 1052 (N–H), 927, 814, 762, 662. ^{1}H NMR (ppm, $CDCl_3$): δ = 7.89–7.52 (m, 16H, Ar–*H*), 7.31–7.21 (m, 16H, Ar–*H*), 7.08–6.84 (m, 12H, Ar–*H*), 3.88–3.82 (t, 16H, O–C*H*$_2$), 3.25–3.16 (t, 16H, N–C*H*$_2$), 2.45 (s, 12H, C*H*$_3$). ^{13}C NMR (ppm, $CDCl_3$): δ = 150.84, 146.78, 144.07, 138.13, 136.60, 130.90, 130.55, 129.90, 129.85, 128.15, 127.74, 123.80, 121.27, 100.95, 66.82–66.73–65.83 (O–*C*H_2), 48.67–48.59 (N–*C*H_2), 21.73–21.63–21.51 (Ar–*C*H_3). Ultraviolet–Visible ($CHCl_3$), λ_{max}, nm (logε): 341 (4.91), 611 (4.41), 646 (4.57), 671 (4.96) and 706 (5.04). Mass Spectra Analysis *m/z*: 1836.05 $[M]^+$.

*2.1.3. Syntheses of metallated phthalocyanines (**6** to **9**)*

The compound **(4)** (0.1 g, 0.244 mmol, 2 eq.) and anhydrous metal salts [$CuCl_2$ (14.76 mg, 0.109 mmol, 1 eq., for **6**); $Zn(OAc)_2$ (22.39 mg, 0.122 mmol, 1 eq., for **7**); $CoCl_2$ (14.15 mg, 0.109 mmol, 1 eq., for **8**) and $MgCl_2$ (11.62 mg, 0.122 mmol, 1 eq., for **9**)] were solvated in dry pentan-1-ol (3.0 mL) inside a Schlenk tube and finally, 6 drops of 1,8-diazabicyclo[5.4.0]undec-7-ene were added. Subsequently, the flask content was purged with nitrogen gas and refluxed at 160 ºC for 12 h for all compounds (**6** to **9**). Followed by chilling to room temperature, the obtained product was precipitated with the addition of 10 mL ethanol and mixed at room temperature for 1 hour. After the filtration of the precipitate, it was then dried under vacuum. Then, it was chromatographed on basic alumina column with chloroform:ethanol solvent system (5.0 mL:5 drops for **6** and **8**); (50.0:5.0 v/v for **7**) and (50.0:1.5 v/v for **9**). The collected solution was condensed in an evaporator to obtain the metallophthalocyanines as blue

(**6** and **8**); dark green (**7**) or light green (**9**) solids. Eventually, the acquired metal complexes were dried *in vacuo*.

2.1.3.1. Peripherally copper (II) phthalocyanine ***(6)***. Color: Blue. Yield: 31.0 mg (29.9%), m.p. >300 ºC. Elemental analysis: Calc. (%) for $C_{100}H_{88}N_{16}O_{12}S_4Cu$: C: 63.29; H: 4.67; N: 11.81; S: 6.76, Found (%) C: 62.41; H: 4.40; N: 11.52; S: 6.47. Fourier Transform–Infrared: υ_{max} (cm^{-1}) = 3045 (Ar C–H), 2955–2920 (C–H), 1607, 1508, 1469, 1449, 1341–1160 (SO_2), 1119 (CH_2–O–CH_2), 926, 812, 764, 659. Ultraviolet–Visible ($CHCl_3$), λ_{max}, nm (logε): 342 (4.64), 618 nm (4.31) and 686 (4.97). Mass Spectra Analysis *m/z*: 1897.76 $[M]^+$.

2.1.3.2. Peripherally zinc (II) phthalocyanine ***(7)***. Color: Dark Green. Yield: 60.0 mg (57.9%), m.p. >300 ºC. Elemental analysis: Calc. (%) for $C_{100}H_{88}N_{16}O_{12}S_4Zn$: C: 63.23; H: 4.67; N: 11.80; S: 6.75, Found (%) C: 62.44; H: 4.60; N: 11.63; S: 6.51. Fourier Transform–Infrared: υ_{max} (cm^{-1}) = 3044 (Ar C–H), 2956–2920 (C–H), 1606, 1509, 1488, 1449, 1332–1159 (SO_2), 1118 (CH_2–O–CH_2), 926, 813, 762, 660. ^{1}H NMR (ppm, $CDCl_3$): δ = 7.81–7.60 (m, 20H, Ar–*H*), 7.30–7.25 (m, 4H, Ar–*H*), 6.85–6.79 (m, 20H, Ar–*H*), 3.79–3.76 (t, 16H, O–C*H*$_2$), 3.16–3.14 (t, 16H, N–C*H*$_2$), 2.48 (s, 12H, C*H*$_3$). ^{13}C NMR (ppm, $CDCl_3$): δ = 150.48, 147.58, 146.58, 143.78, 143.33, 140.56, 137.68, 136.30, 132.96, 130.29, 129.87, 129.74, 128.11, 124.63, 120.84, 112.16, 105.82, 102.30, 100.97, 66.85–66.77– 66.56–65.83 (O–*C*H_2), 48.94–48.54–48.42 (N–*C*H_2), 22.68–22.59–21.70–21.52–20.81 (Ar–*C*H_3). Ultraviolet–Visible ($CHCl_3$), λ_{max}, nm (logε): 350 (4.60), 617 (4.28) and 684 (4.99). Mass Spectra Analysis *m/z*: 1899.62 $[M]^+$.

2.1.3.3. Peripherally cobalt (II) phthalocyanine ***(8)***. Color: Blue. Yield: 12.0 mg (11.6%), m.p. >300 ºC. Elemental analysis: Calc. (%) for $C_{100}H_{88}N_{16}O_{12}S_4Co$: C: 63.45; H: 4.69; N: 11.84; S: 6.78, Found (%) C: 62.68; H: 4.47; N: 11.63; S: 6.54. Fourier Transform–Infrared: υ_{max} (cm^{-1}) = 3048 (Ar C–H), 2956–2915 (C–H), 1604, 1508, 1449, 1346–1160 (SO_2), 1119 (CH_2–O–CH_2), 926, 813, 765, 660. Ultraviolet–Visible ($CHCl_3$), λ_{max}, nm (logε): 332 (4.90), 618 nm (4.52) and 680 (5.03). Mass Spectra Analysis *m/z*: 1893.91 $[M]^+$.

2.1.3.4. Peripherally magnesium (II) phthalocyanine ***(9)***. Color: Light Green. Yield: 40.0 mg (39.5%), m.p. >300 ºC. Elemental analysis: Calc. (%) for $C_{100}H_{88}N_{16}O_{12}S_4Mg$: C: 64.63; H: 4.77;

N: 12.06; S: 6.90, Found (%) C: 64.26; H: 4.62; N: 11.74; S: 6.62. Fouirer Transform–Infrared: υ_{max} (cm^{-1}) = 3044 (Ar C–H), 2956–2917–2894 (C–H), 1606, 1509, 1483, 1332–1159 (SO_2), 1234, 1119 (CH_2–O–CH_2), 926, 813, 752, 661. ^{1}H NMR (ppm, $CDCl_3$): δ = 7.75–7.53 (m, 22H, Ar–*H*), 7.31–7.25 (m, 4H, Ar–*H*), 6.91–6.78 (m, 18H, Ar–*H*), 3.89–3.82 (t, 16H, O–C*H*$_2$), 3.18–3.15 (t, 16H, N–C*H*$_2$), 2.46 (s, 12H, C*H*$_3$). ^{13}C NMR (ppm, $CDCl_3$): δ = 150.63, 148.82, 148.24, 144.22, 143.76, 142.93, 139.56, 139.44, 137.62, 132.91, 132.62, 130.41, 129.79, 129.71, 128.02, 126.19, 123.37, 104.86, 103.63, 66.74–65.83 (O–*C*H_2), 48.67 (N–*C*H_2), 21.68 (Ar–*C*H_3). Ultraviolet–Visible ($CHCI_3$), λ_{max}, nm (logε): 355 (4.57), 619 (4.27) and 686 (5.00). Mass Spectra Analysis *m/z*: 1858.37 $[M]^+$.

3. Results and discussion

3.1. Syntheses and characterization

In Scheme, the syntheses route associated with the tosylated 4-morpholinoaniline functionalities fused at the peripheral positions of phthalonitrile compound **(4)** and their corresponding free-base **(5)**, copper(II) **(6)**, zinc(II) **(7)**, cobalt(II) **(8)** and magnesium(II) **(9)** Pcs were demonstrated. In this work, the synthesis, structural verification, DNA cleavage effects of the new phthalocyaninato copper(II) **(6)**, zinc(II) **(7)**, cobalt(II) **(8)** and magnesium(II) **(9)** compounds were reported. Compound **(7)** which had the best photocleavage effects among tested compounds was investigated DNA binding effect and singlet oxygen quantum yield using UV-vis spectroscopy. Also, cytotoxic and phototoxic properties of compound **(7)** against human colorectal (HCT-116) and cervical (HeLa) cancer cells were investigated using MTT assay. The main goal of this research was to acquire new potent photosensitizing agents for PDT applications for the treatment of cancerous tumors. Common spectroscopic techniques such as Fourier Transform–Infrared (Attenuated Total Reflection sampling accessory), Matrix Assisted Laser Desorption/Ionization–Time of Flight Mass spectral data (Dithranol, abbreviated as DIT used as the matrix), elemental analysis, Ultraviolet-Visible (UV–vis), ^{1}H NMR and ^{13}C NMR were utilized for the verification of the newly synthesized chemical structures and the results were found in accordance with the proposed chemical structures in Scheme.

In the first step, we prepared the tosylated 4-morpholinoaniline compound **(2** *via* the reaction of 4-morpholinoaniline **(1)** and Ts–CI in dry pyridine at –5 ºC with 68.8% yield through the modification of the synthetic method cited in the literature [56]. Then, the dicyano compound **(4)** which was the starting reagent for the corresponding free-base **(5)** and its metallophthalocyanines (**6** to **9**) were synthesized by the reaction of 4-nitrophthalonitrile **(3)** with compound **(2)** and anhydrous K_2CO_3 in dry DMF with 79.1% yield. Following that, free-base **(5)** was synthesized from the dicyano compound **(4)** in the presence of the catalytic amount of DBU in dry pentan-1-ol at 160 °C under nitrogen stream inside a Schlenk tube. And lastly, the Cu^{II} **(6)**, Zn^{II} **(7)**, Co^{II} **(8)** and Mg^{II} **(9)** Pcs were synthesized as blue (**6** and **8**); dark green (**7**) or light green (**9**) solids *via* cyclotetramerization reaction of (**4**) in the existence of anhydrous salts [CuI_2 for **(6)**, $Zn(CH_3COO)_2$ for **(7),** CoI_2 for **(8)** and $MgCI_2$ for **(9)**] with 6 drops of DBU as the strong base in dry pentan-1-ol at 160 °C inside a Schlenk tube connected with N_2(g) gas. The newly prepared metallophthalocyanines **(6** to **9)** were chromatographed on the basic alumina column with chloroform:ethanol solvent systems given in the experimental section for final purification whereas the free-base Pc **(5)** was purified by washing the crude product with hot ethanol. The unsubstituted phthalocyanines (free-bases and metallophthalocyanines) generally do not dissolve in most of the solvents. All the new phthalocyanine metal complexes **(5** to **9)** synthesized for this study were soluble in common organic solvents including tetrahydrofuran, chloroform, dichloromethane, ethyl acetate, dimethylsulfoxide and *N,N*-dimethylformamide owing to the substitution of four tosylated 4-morpholinoaniline functionalities at peripheral sites of phthalocyanine scaffold.

The N–H vibration peaks at 3154 cm^{-1} and 1051 cm^{-1} in the FT–IR spectra of the compound **(2)** disappeared after the synthesis of the peripheral dicyano derivative (**4)** and a new vibration peak arose at 2228 cm^{-1} which was ascribed to the formation of C≡N functionality. The aromatic C–H stretchings were monitored at 3078–3051 cm^{-1}; aliphatic C–H stretches at 2973–2920–2887 cm^{-1}; the tosyl group (S=O asymmetric and symmetric vibrations) at 1361–1159 cm^{-1} for the compound (**4**). Other characteristic FT–IR vibration peaks concerning the compound **(4)** were similar to starting compound **(2)** with small changes. In the ^{1}H NMR spectra of dicyano derivative **(4),** a singlet N–H proton signal, integrating 1 proton, of the tosylated compound **(2)** at δ = 6.79 ppm vanished. As expected, aromatic protons were resonated at δ = 7.65–7.43, 7.34–7.23 and 7.03–6.78 ppm. The signals of CH_2 and methyl protons were resonated at δ = 3.88–3.86

(O–CH_2), 3.25–3.22 (N–CH_2) and 2.46–2.45 ppm (CH_3) in the ^{1}H NMR spectra of compound **(4)**. The observation of the signals in ^{13}C NMR spectra belonging to the *C*≡N functionalities at δ = 115.82–115.81–115.24–115.07 ppm was proved the proposed compound **(4)**. The aromatic carbon signals of phthalonitrile derivative **(4)** were observed between at δ = 151.68 and 110.24 ppm. Other ^{13}C NMR signals of the compound **(4)** were observed at δ = 66.66–66.65–65.84 ppm (O–*C*H_2), 48.19–48.18 ppm (N–*C*H_2) and 21.67–21.66 ppm (Ar–*C*H_3) (Figure 1). The Mass Spectra Analysis data of the compound **(4)** was measured *via* MALDI–TOF–MS technique and at *m/z*: value was detected as 458.21 $[M]^+$. All spectral data were in good accord with the newly synthesized precursor compound **(4)**.

To confirm the structural characterization of the new free-base phthalocyanine **(5)**, we firstly evaluated the disappearance of the sharp C≡N vibrations at 2228 cm^{-1} in the Fourier transform infrared spectrum of dicyano compound **(4)**. Besides, a new stretching vibration was monitored in the FT–IR spectrum of **(5)** at 3292 and 1052 cm^{-1} belonging to the secondary amine (N–H) functionalities inside the inner core of phthalocyanine ring. The rest of the FT–IR spectrum of **(5)** had a similarity to that of the starting phthalonitrile compound **(4)** with slight vibrational variations. The proton signals of aromatic rings in the ^{1}H NMR spectrum of **(5)** were detected at 7.89–7.52, 7.31–7.21 and 7.08–6.84 ppm. The CH_2 and methyl protons were monitored at 3.88–3.82 (O–CH_2), 3.25–3.16 (N–CH_2), 2.45 ppm (CH_3), respectively. With small changes in chemical shifts, the ^{1}H NMR signals of **(5)** were similar to that of the precursor phthalonitrile compound **(4)**. During the NMR measurements, a common feature of the ^{1}H NMR spectra of the free-base Pc molecules is the broad absorption that is occurred most likely through the strong aggregation of free-base Pc, which is most likely taken place at the concentration used for ^{1}H NMR samples [57–59]. The two inner core protons of free-base phthalocyanine **(5)** could not be observed because of this broad absorption that is presumably happened through the strong aggregation between phthalocyanine molecules in the deuterated chloroform during the preparation and measurement of NMR samples [60,61]. In the case of ^{13}C NMR spectrum of free-base phthalocyanine **(5)**, the C≡N functional groups for the dicyano compound **(4)** at δ = 115.82–115.81–115.24–115.07 ppm disappeared. ^{13}C NMR signals of the phthalocyanine **(5)** given in the experimental section exhibited a resemblance to that of the dicyano compound **(4)**. The molecular ion peak was observed at *m/z* = 1836.05 $[M]^+$ in the Mass Spectra Analysis data of **(5)** (Figure 2).

As we compared the infrared spectrum of dicyano derivative **(4)** with Cu^{II} **(6)**, Zn^{II} **(7)**, Co^{II} **(8)** and Mg^{II} **(9)** phthalocyanines, the disappearance of C≡N vibration of compound **(4)** indicated that the cyclotetramerization reactions from phthalonitrile derivatives to corresponding metallophthalocyanines **(6–9)** were succeeded. Other vibrational bands of phthalocyanine metal complexes **(6** to **9)** were alike to the FT–IR spectrum of corresponding phthalonitrile derivative **(4)** with small changes. In the ^{1}H NMR spectra of peripheral zinc(II) **(7)** and magnesium(II) **(9)** phthalocyanines, aromatic protons were resonated at δ = 7.81–7.60, 7.30–7.25 and 6.85–6.79 ppm for **(7)**; 7.75–7.53, 7.31–7.25 and 6.91–6.78 ppm for **(9)**. Other proton signals were monitored at δ = 3.79–3.76 (O–C*H*$_2$), 3.16–3.14 (N–C*H*$_2$) and 2.48 (C*H*$_3$) ppm for **(7)**; 3.89–3.82 (O–C*H*$_2$), 3.18–3.15 (N–C*H*$_2$) and 2.46 (C*H*$_3$) ppm for **(9)**. When we compare the ^{13}C NMR spectra of compounds (**7** and **9**) with corresponding dicyano compound **(4)**, the *C*≡N signals of **(4)** at δ = 115.82–115.81–115.24–115.07 ppm were disappeared, indicating that the targeted metal complexes were successfully synthesized from their dicyano derivative **(4)**. Aromatic carbon signals were resonated between at δ = 150.48 and 100.97 ppm for **(7)**; 150.63 and 103.63 ppm for **(9)**, respectively. Other ^{13}C NMR signals were as flows: 66.85–66.77–66.56–65.83 (O–*C*H$_2$), 48.94–48.54–48.42 (N–*C*H$_2$) and 22.68–22.59–21.70–21.52–20.81 ppm (Ar–*C*H$_3$) for **(7)**; 66.74–65.83 (O–*C*H$_2$), 48.67 (N–*C*H$_2$) and 21.68 ppm (Ar–*C*H$_3$) for **(9)**. According to the Mass Spectra Analysis data of the metallated phthalocyanine derivatives, the *m/z*: values were observed at 1897.11 $[M]^+$ for **(6)**; 1893.23 $[M]^+$ for **(8)**; 1899.62 $[M]^+$ for **(7)** and 1858.37 $[M]^+$ for **(9)** (Figure 3). All spectral data supported the newly synthesized phthalocyaninato copper(II) **(6)**, zinc(II) **(7)**, cobalt(II) **(8)** and magnesium(II) **(9)** Pcs.

3.2. Ultraviolet-visible spectra

As it is known, one of the best verification methods for the formation of phthalocyanines is obtained from UV–vis spectral measurements. To do so, we benefited from ground state electronic spectra of newly synthesized free-base **(5)**, Cu^{II} **(6)**, Zn^{II} **(7)**, Co^{II} **(8)** and Mg^{II} **(9)** Pcs (C = 1.0×10^{-5} M) in chloroform in addition to aforementioned spectral techniques. As expected, free-base Pc **(5)** showed two split Q Bands (Q_x and Q_x) with high intensity which was typical with Ultraviolet-visible (UV–vis*)* spectra of free-base phthalocyanines with D_{2h} symmetry. The Q band and B band absorptions in the electronic absorption spectrum of compound **(5)** are as

follows: 706 nm (logε = 5.04) (Q_x), 671 nm (logε = 4.96) (Q_y), 646 nm (logε = 4.57), 611 nm (logε = 4.41) and 341 nm (logε = 4.91) (Figure 4). The ground state electronic spectra of compounds (**6** to **9**) recorded as the typical of metallated phthalocyanines with a single band of high intensity at 686 nm (logε = 4.97) and 618 nm (logε = 4.31) for **(6)**; 684 nm (logε = 4.99) and 617 nm (logε = 4.28) for **(7)**; 680 nm (logε = 5.03) and 618 nm (logε = 4.52) for **(8)**; 686 nm (logε = 5.00) and 619 nm (logε = 4.27) for **(9)**, respectively. Along with Q band absorption, the studied metallophthalocyanines (**6** to **9**) displayed B band absorptions in the Soret region at 342 nm (logε = 4.64) for **(6)**; 350 nm (logε = 4.60) for **(7)**; 332 nm (logε = 4.90) for **(8)** and 355 nm (logε = 4.57) for **(9)** as well. The UV–vis spectral measurements were consistent with the proposed phthalocyanine compounds (**5** to **9**) (Figure 4).

3.3. DNA cleavage studies

The DNA cleavage assays were carried out as described previously with minor modifications [62]. The pBR322 plasmid DNA (Thermo Fischer Scientific, SD0041) cleavage activities of the compounds (**6**–**9**) were investigated on agarose gel electrophoresis and analyzed using Image Lab Version 4.0.1 Software. The results of cleavage activities of the compounds (**6**–**9**) without and with irradiation were given in Figures 5 and 6. The compounds (**6**–**9**) did not show cleavage activities in the dark, as shown in Figure 5. The results suggested that the compounds had a low cytotoxic effect in the dark, which is very important for acting as the photosensitizer. On the other hand, compound **(7)** cleaved pBR322 plasmid DNA with light irradiation (white, 17.5 mW/cm^2, 30 min) showing that DNA cleavage from supercoiled form to nicked form as shown in Figure 6, Lane 5–7. The untreated pBR322 plasmid DNA was determined as 97.40% (supercoiled form) and 2.60% (nicked form) with irradiation under our experimental conditions. Upon increasing concentration of the compound **(7)** (25, 50 and 100 µM) with plasmid DNA, the nicked form increased from 2.60% to 41.10%. The other tested compounds (**6**, **8** and **9**) did not show any photocleavage effects under our experimental conditions. It is well-known that zinc(II) compounds have high singlet oxygen quantum yield due to d^{10} configuration [63]. Therefore, compound **(7)** might show photocleavage activities *via* a singlet oxygen pathway against plasmid DNA.

3.4. DNA binding studies of Zn(II) phthalocyanine derivative (7)

UV-vis spectroscopy is an important technique to estimate the binding mode of compounds with calf-thymus DNA (ct-DNA). It is well-known that compounds interact with DNA *via* covalent or non-covalent (intercalation, major/minor groove binding and electrostatic) bonds. The spectral changes with the interaction of compounds with ct-DNA show the binding propensity in the UV-vis spectrum [62]. Compound **(7)** showed a hypochromic effect (25.98%) without any shift upon the addition of increasing concentrations of ct-DNA. Also, the intrinsic binding constant (K_b) of compound **(7)** was determined as 2.45 ± (0.20) × 10^4 M^{-1}. In our previous studies, K_b values of tetra 4-(3-methyl-4-(3-morpholinopropyl)-5-oxo-4,5-dihydro-1H-1,2,4-triazol-1-yl) substituted Zn(II) and morpholine substituted Zn(II) phthalocyanines were calculated as 6.53 ± (0.04) × 10^4 and 4.76 (± 0.06) × 10^4 M^{-1}, respectively [62,63]. Compound **(7)** had a lower binding affinity than our previous studies due to the bulky structure. UV-vis spectroscopy studies showed that compound **(7)** bound to ct-DNA *via* non-covalent interaction.

*3.5. Photochemical parameters of Zn(II) phthalocyanine derivative **(7)***

One of the most important parameters for PDT applications of a photosensitizer is the singlet oxygen quantum yield (Φ_Δ) [64]. In the present study, singlet oxygen quantum yield (Φ_Δ) of compound **(7)** in DMF was calculated with 1,3-diphenylisobenzofuran (DPBF) used as a singlet oxygen quencher. The absorption decay of DPBF was monitored at 417 nm using a UV-vis spectrophotometer during irradiation. The results were shown in Table 1 and Figure 7. Figure 7 showed that absorbance of the DPBF decreased at 417 nm due to singlet oxygen, but Q band shapes of compound **(7)** did not change. This behavior showed that compound **(7)** was stable against light irradiation. The Φ_Δ value of compound **(7)** was determined as 0.11, while unsubstituted ZnPc was 0.56 in DMF.

*3.6. Cytotoxicity and phototoxicity of Zn(II) phthalocyanine derivative **(7)***

In this study, cytotoxicity and phototoxicity of the compound **(7)** which showed the best photocleavage effects among tested compounds were examined using MTT assay against HCT-

116 and HeLa cancer cells with/without irradiation. In this test, the water-soluble yellowish MTT dye is metabolized by succinate dehydrogenase enzyme in the viable active cells; and produces water-insoluble purple formazan crystals. This color change is used as an indicator of cell viability [65]. The results were tabulated in Tables 2, 3 and Figures 8, 9. Table 2 showed that cell viabilities of HCT-116 cells (%) at 50 and 100 µM of compound **(7)** were determined as 90 ± 1.30% and 73 ± 1.60%, respectively with irradiation (white, 17.5 mW/cm^2, 1 h). In the dark, they were found to be 93 ± 2.50% and 85 ± 4.40%, respectively. On the other hand, compound **(7)** on HeLa cells had higher phototoxic activity than HCT-116 cells. Upon irradiation, cell viabilities of HeLa cells (%) were 83 ± 3.80%, 71 ± 1.70% and 65 ± 2.50%, respectively at 10, 50 and 100 µM. As shown in Table 3, cell viabilities were determined as 90 ± 4.80%, 74 ± 2.00% and 69 ± 1.60% at same concentrations in the dark At 1 and 5 µM, compound **(7)** did not any cytotoxic and phototoxic effects against HCT-116 and HeLa cells with/without irradiation.

In the previous studies demonstrated that quaternized 2, 9(10), 16(17), 23(24)-tetra-(4-(N-propanesulfonic-acid) phenoxy) phthalocyaninto-zinc(II), non-ionic (2, 9(10), 16(17), 23(24)-tetra-(4-(N-(2-methyls)) phenoxy) phthalocyaninato-zinc(II), and cationic (2, 9(10), 16(17), 23(24)-tetra-(4-(N-(2-methyls)) phenoxy) phthalocyaninato-zinc(II) showed phototoxic effects on HeLa cells upon irradiation (665 nm LED) in a time-dependent manner [66]. Besides, Göksel reported that the determined IC_{50} values for zinc(II) phthalocyanine containing [2-(tert-butoxycarbonyl)amino]ethoxy and iodine groups on HeLa cells were 4.5 and 2.17 µM after irradiation with 2 J.cm^{-2} due to high singlet oxygen quantum yields [67]. Moreover, tetra-triethyleneoxysulfonyl substituted zinc phthalocyanine had phototoxic activities against HCT-116 cells with a broadband white light source at 10 J.cm^{-2} [68]. Comparing previous studies and our studies, compound **(7)** had lower cytotoxic and phototoxic activities on HCT-116 and HeLa cells despite effective DNA cleavage properties of it. This may trigger by the low cellular uptake and intracellular reactive oxygen species due to its large structure. Several studies demonstrated that the drug carrier system was helpful for phthalocyanines to uptake cells and improve their activity.

4. Conclusion

The synthetic procedures and chemical characterization of the new peripherally tosylated 4-morpholinoaniline functionalities attached to phthalocyanines were announced in this report.

The newly synthesized compounds were verified *via* elemental analysis, Fourier Transform–Infrared, Matrix Assisted Laser Desorption/Ionization–Time of Flight Mass spectral data, ^{1}H NMR and ^{13}C NMR, and as well as UV–vis. Due to the tosylated substituents at peripheral and sites of phthalocyanine skeleton, these new tetra-substituted phthalocyanines (**5** to **9**) showed good solubility in common organic solvents such as dimethylformamide, chloroform, tetrahydrofuran, ethanol, dichloromethane, ethyl acetate, and dimethyl sulfoxide. The UV–vis spectra of studied metallophthalocyanines **(6–9)** were recorded at room temperature with 1.00 x 10^{-5} M concentration in chloroform. Depending on the electronic absorption spectra, we obtained monomeric species with D_{4h} symmetry, as evidenced by a single narrow Q band with a short wavelength shoulder in terms of working conditions.

The potential utilization of the new peripheral phthalocyanine compounds (**6** to **9**) as the new pharmaceutical agents in PDT applications were determined in DMSO in aspects of pBR322 plasmid DNA cleavage on agarose gel electrophoresis. The results showed that compound **(7)** cleaved significantly pBR322 plasmid DNA upon irradiation. Compound **(7)** displayed a hypochromic effect without any shift on the addition of increasing concentrations of ct-DNA and K_b of compound **(7)** was calculated as $2.45 \pm (0.20) \times 10^4\ M^{-1}$. In photochemical studies, the Φ_Δ value of compound **(7)** was determined as 0.11. The cytotoxicity and phototoxicity effects of compound **(7)** were investigated using MTT assay on HCT-116 and HeLa cancer cells. The compound **(7)** had a low cytotoxic and phototoxic effect against used cancer cell lines because this may trigger by the low cellular uptake and intracellular reactive oxygen species due to its large structure. Further studies are required to determine the potential therapeutic effect of compound (**7**) using a drug carrier system such as nanoparticles liposomes and micelles etc.

References

[1] H. Ali, J.E. van Lier, Chem. Rev. 99 (1999) 2379–2450.

[2] J. Jeong, R.S. Kumar, N. Mergu, Y.-A. Son, J. Mol. Struct. 1147 (2017) 469–479.

[3] P. Gregory, J. Porphyrins Phthalocyanines 4 (2000) 432–437.

[4] C.G. Claessens, U. Hahn, T. Torres, Chem. Rec. 8 (2008) 75–97.

[5] T. Nyokong, E. Antunes, in: K.M. Kadish, K.M. Smith, R. Guilard (Eds.), Handbook of Porphyrin Science, vol. 7, World Scientific, New Jersey, 2010, p. 247.

[6] A. Nas, Ü. Demirbaş, M. Pişkin, M. Durmuş, H. Kantekin, J. Lumin. 145 (2014) 635-642.

[7] Ü. Demirbaş, M. Pişkin, B. Barut, R. Bayrak, M. Durmuş, H. Kantekin, Synth. Met. 220 (2016) 276-285.

[8] E. Ranyuk, R. Lebel, Y. Bérubé-Lauziére, K. Klarskov, R. Lecomte, J.E. van Lier, B. Guérin, Bioconjugate Chem. 24 (2013) 1624–1633.

[9] A. Galstyan, D. Block, S. Niemann, M.C. Grüner, S. Abbruzzetti, M. Oneto, C. G. Daniliuc, S. Hermann, C. Viappiani, M. Schäfers, B. Löffler, C.A. Strassert, A. Faust, Chem. Eur. J. 22 (2016) 5243–5252.

[10] Y. Zhang, J.F. Lovell, WIREs Nanomed. Nanobiotechnol. 9 (2017) e1420.

[11] M.–E. Ragoussi, M. Ince, T. Torres, Eur. J. Org. Chem. (2013) 6475–6489.

[12] A. Günsel, E. Güzel, A.T. Bilgiçli, İ. Şişman, M.N. Yarasir, J. Photochem. Photobiol. A Chem. 348 (2017) 57–67.

[13] Z.Z. Özturk, N. Kılınc, D. Atilla, A.G. Gurek, V. Ahsen, J. Porphyrins Phthalocyanines 13 (2009) 1179–1187.

[14] M. Bouvet, P. Gaudillat, J.M. Suisse, J. Porphyrins Phthalocyanines 17 (2013) 913–919.

[15] M. Gsänger, D. Bialas, L. Huang, M. Stolte, F. Würthnew, Adv. Mater. 28 (2016) 3615–3645.

[16] S.R. Nxele, T. Nyokong, Electrochim. Acta 194 (2016) 26–39.

[17] M.M. Nicholson, in: C.C. Leznoff, A.B.P. Lever (Eds.), Phthalocyanines Properties and Applications, vol. 3, VCH Publisher, New York, 1993, p. 71.

[18] D.S. Weiss, J. Image. Sci. Tech. 60 (2016) 30505-1-30505-24(24).

[19] B. Zhu, X. Zhang, M. Han, P. Deng, Q. Li, J. Mol. Struct. 1079 (2015) 61–66.

[20] A.M. Sevim, C. Ilgün, A. Gül, Dyes Pigm. 89 (2011) 162–168.

[21] J.B. Hester, E.G. Nidy, S.C. Perricone, T.J. Poel, PCT Int. Appl. (2001). W00144188.

[22] R.S. Varma, R. Prakash, M.M. Khan, A. Ali, Indian Drugs 23 (1986) 345–349.

[23] M.G. Verma, V.R. Sharma, A.K. Saxena, T.N. Bhalla, J.N.S. Inha, K.P. Bhargava, Pharmacol. Res. Commun. 16 (1984) 9–20.

[24] R. Agarwal, C. Agarwal, S. Singh, V.S. Misra, J. Chem. Soc. Pak. 6 (1984) 84–94.

[25] V.S. Misra, S. Singh, R. Agarwal, K.C. Chaudhary, J. Chem. Soc. Pak. 3 (1981) 209–213.

[26] M.D. Deshmukh, A.G. Doshi, J. Orient. Chem. 11 (1995) 85–86.

[27] S.K. Sridhar, M. Saravanan, A. Ramesh, Eur. J. Med. Chem. 36 (2001) 615–625.

[28] R. Agarwal, K.C. Chaudhary, V.S. Misra, J. Indian Chem. 22B (1983) 308–310.

[29] R.S. Varma, R. Prakash, C.R. Prasad, J. Chem. Soc. Pak. 8 (1986) 117–123.

[30] M.-J. Camarasa, Heterocyclic chemistry in drug discovery, in: Jie Jack Li (Ed.), ChemMedChem. 9 (2014) 233–234.

[31] W. Zhu, C. Sun, S. Xu, C. Wu, J. Wu, M. Xu, H. Zhao, L. Chen, W. Zeng, P. Zheng, Bioorg. Med. Chem. 22 (2014) 6746–6754.

[32] K. Dhahagani, S. Mathan Kumar, G. Chakkaravarthi, K. Anitha, J. Rajesh, A. Ramu, G. Rajagopal, Spectrochim. Acta Part A: Mol. Biomol. Spect. 117 (2014) 87–94.

[33] H. Enzmann, H. Zerban, A. Kopp-Schneider, E. Löser, P. Bannasch, Carcinogenesis 16 (1995) 1513–1518.

[34] R.J. Lewis Sr., Danger Prop. Ind. Mater. Rep. 15 (1995) 270–297.

[35] T. V Abramova, P.A. Bakharev, S. V Vasilyeva, V.N. Silnikov, Tetrahedron Lett. 45 (2004) 4361–4364.

[36] M.L. Leathen, B.R. Rosen, J.P. Wolfe, J. Org. Chem. 74 (2009) 5107–5110.

[37] Z. Yu, G. Shi, Q. Sun, H. Jin, Y. Teng, K. Tao, G. Zhou, W. Liu, F. Wen, T. Hou, Eur. J. Med. Chem. 44 (2009) 4726–4733.

[38] A.D. Tereshchenko, J.S. Myronchuk, L.D. Leitchenko, I.V. Knysh, G.O. Tokmakova, O.O. Litsis, A. Tolmachev, K. Liubchak, P. Mykhailiuk, Tetrahedron 73 (2017) 750–757.

[39] B. Barut, Ü. Demirbaş, A. Şenocak, A. Özel, H. Kantekin, Synth. Met. 229 (2017) 22–32.

[40] A.K. Burat, A. Koca, J.P. Lewtak, D.T. Gryko, Synth. Met. 161 (2011) 1537–1545.

[41] S. Çolak, M. Durmuş, S.Z. Yıldız, J. Photochem. Photobiol. A Chem. 325 (2016) 125–134.

[42] J. Dlugaszewska, W. Szczolko, T. Koczorowski, P. Skupin-Mrugalska, A. Teubert, K. Konopka, M. Kucinska, M. Murias, N. Düzgüneş, J. Mielcarek, T. Goslinski, J. Inorg. Biochem. 172 (2017) 67–79.

[43] C. Duncan, A.R. White, Metallomics 4 (2012) 127–138.

[44] C.Y. Ang, S.Y. Tan, Y.Zhao, Org. Biomol. Chem. 12 (2014) 4776–4806.

[45] O. Laccourreye, A. Werner, L. Laccourreye, P. Bonfils, Eur. Ann. Otorhinolaryngol. Head Neck Dis. 134 (2017) 95–99.

[46] P. García-García, F. López-Muñoz, G. Rubio, B. Martín-Agueda, C. Alamo, Phytomedicine 15 (2008) 566–576.

[47] Ü. Demirbaş, C. Göl, B. Barut, R. Bayrak, M. Durmuş, H. Kantekin, J. Mol. Struc. 1130 (2017) 677-687.

[48] A.C. Kubler, Photodynamic therapy, Med. Laser Appl. 20 (2005) 37–45.

[49] A. Mitra, G.I. Stables, Photodiag. Photodyn. Ther. 3 (2006) 116–127.

[50] T.J. Dougherty, C.J. Gomer, B.W. Henderson, G. Jori, D. Kessel, M. Korbelik, J. Moan, Q. Peng, J. Natl. Cancer Inst. 90 (1998) 889–905.

[51] R.R. Allison, K. Moghissi, Clin. Endosc. 46 (2013) 24–29.

[52] M. Ochsner, J. Photochem. Photobiol. B Biol. 39 (1997) 1–18.

[53] P. Agostinis, K. Berg, K.A. Cengel, T.H. Foster, A.W. Girotti, S.O. Gollnick, S.M. Hahn, M.R. Hamblin, A. Juzeniene, D. Kessel, M. Korbelik, J. Moan, P. Mroz, D. Nowis, J. Piette, B.C. Wilson, J. Golab, CA Cancer J. Clin. 61(4) (2011) 250–281.

[54] H. Yalazan, B. Barut, G. Sarkı, B. Ertem, Y. Ünver, A. Özel, H. Kantekin, , J. Coord. Chem. 72(14) (2019) 2409–2421.

[55] J.G. Young, W. Onyebuagu, J. Org. Chem. 55 (1990) 2155–2159.

[56] M. Koçak, A.İ. Okur, Ö. Bekaroğlu, J. Chem. Soc., Dalton Trans. (1994) 323–326.

[57] S.Z. Yıldız, Y. Gök, N. J. Chem. 22 (1998) 1365–1369.

[58] M. Hanack, H. Heckmann, R. Polley, Methods of Organic Chemistry, Additional Supplementary Volume, Georg Thieme Verlag, Stuttgart, 1998.

[59] Y. Gök, H. Kantekin, I. Degirmencioğlu, Supramol. Chem. 15 (2003) 335–343.

[60] A. Bilgin, B. Ertem, Y. Gök, Tetrahedron Lett. 44(19) (2003) 3829–3833.

[61] C.F. van Nostrum, S.J. Picken, A.-J. Schouten, R. J. M. Nolte, J. Am. Chem. Soc. 117(40) (1995) 9957–9965.

[62] A. Özel, Ü. Demirbaş, B. Barut, H. Kantekin, J. Mol. Struc. 1186 (2019) 325–332.

[63] B. Barut, Ü. Demirbaş, A. Özel, H. Kantekin, Int. J. Biol. Macromol. 105 (2017) 499–508.

[64] B. Barut, C.Ö. Yalçın, S. Sarı, Ö. Çoban, T. Keleş, Z. Bıyıklıoğlu, M. Abudayyak, Ü. Demirbaş, A. Özel, Eur. J. Med. Chem. 183 (2019) 111685.

[65] M. Abudayyak, E. Güzel, G. Özhan, Neurochem. Int. 108 (2017) 7–14.

[66] L. Gui, Q. Zhang, Y. Wang, K. Fang, A. Wang, X. You, L. Zhou, J. Zhou, S. Wei, Inorg. Chem. Commun. 75 (2017) 1–4.

[67] M. Göksel, Bioorg. Med. Chem. 24 (2016) 4152–4164.

[68] W. Kuzyniak, E. Ermilov, D. Atilla, A. Gürek, B. Nitzsche, K. Derkow, B. Hoffman, G. Steinemann, V. Ahsen, M. Höpfner, Photodiagn. Photodyn. Ther. 13 (2016) 148–157.

Table Captions

Table 1. Maximum electronic absorption and singlet oxygen quantum yield for zinc(II) phthalocyanine **(7)** in DMF.

Table 2. Cytotoxic and phototoxic effects of compound **(7)** on HCT-116 cells expressed as cell viability (%).

Table 3. Cytotoxic and phototoxic effects of compound **(7)** on HeLa cells expressed as cell viability (%).

Table 1. Maximum electronic absorption and singlet oxygen quantum yield for zinc(II) phthalocyanine **(7)** in DMF.

Compound	**Solvent**	**Q band λ_{max}, (nm)**	**(log ε)**	**Φ_Δ**
ZnPc **(7)**	DMF	683	5.28	0.11
ZnPc[a]	DMF	670	5.37	0.56

[a] Tetrahedron, 2010, 66, 3248–3258.

Table 2. Cytotoxic and phototoxic effects of compound **(7)** on HCT-116 cells expressed as cell viability (%).

	1 µM	**5 µM**	**10 µM**	**50 µM**	**100 µM**
(7) without irradiation	100 ± 3.10	100 ±1.50	100 ± 1.50	93 ± 2.50	85 ± 4.40
(7) with irradiation	100 ± 2.90 ^{ns}	100 ± 0.90 ^{ns}	100 ± 0.70 ^{ns}	90 ± 1.30^{ns}	73 ± 1.60***

*** $p < 0.001$, ns: not significant compared to without irradiation at the same concentration.

Table 3. Cytotoxic and phototoxic effects of compound **(7)** on HeLa cells expressed as cell viability (%).

	1 µM	**5 µM**	**10 µM**	**50 µM**	**100 µM**
(**7**) without irradiation	100 ± 4.60	100 ± 2.50	90 ± 4.80	74 ± 2.00	69 ± 1.60
(**7**) with irradiation	100 ± 1.30 ^{ns}	100 ± 2.30 ^{ns}	83 ± 3.80 ^{ns}	71 ± 1.70^{ns}	65 ± 5.50^{ns}

ns: not significant compared to without irradiation at the same concentration.

Scheme and Figure Captions

Scheme. The synthesis of the peripheral tetra-substituted free-base **(5)**, copper(II) **(6)**, zinc(II) **(7)**, cobalt(II) **(8)** and magnesium(II) **(9)** phthalocyanine derivatives.

Figure 1. ^{1}H and ^{13}C NMR spectra of the precursor dicyano compound **(4)** in $CDCI_3$.

Figure 2. Mass spectral data of the compounds **(2)** and **(5)**.

Figure 3. Mass spectral data of the compounds **(7)** and **(9)**.

Figure 4. The ground state electronic absorption spectra of new free-base **(5)** copper(II) **(6)**, zinc(II) **(7)**, cobalt(II) **(8)** and magnesium(II) **(9)** phthalocyanines (C = 1.0×10^{-5} M) in chloroform.

Figure 5. Agarose gel electrophoresis of pBR322 plasmid DNA in the absence and presence of compounds without irradiation. Lane 1, DNA control; lane 2–4, **(6)** (25, 50 and 100 μM); lane 5–7, **(7)** (25, 50 and 100 μM); lane 8–10, **(8)** (25, 50 and 100 μM); lane 11–13, **(9)** (25, 50 and 100 μM).

Figure 6. Agarose gel electrophoresis of pBR322 plasmid DNA in the absence and presence of compounds with irradiation (white, 17.5 mW/cm^2, 30 min). Lane 1, DNA control; lane 2–4, **(6)** (25, 50 and 100 μM); lane 5–7, **(7)** (25, 50 and 100 μM); lane 8–10, **(8)** (25, 50 and 100 μM); lane 11–13, **(9)** (25, 50 and 100 μM).

Figure 7. Absorption changes during the determination of singlet oxygen quantum yield for zinc(II) phthalocyanine **(7)** in DMF using DPBF as a singlet oxygen quencher.

Figure 8. Cytotoxic and phototoxic effects of zinc(II) phthalocyanine **(7)** against HCT-116.

Figure 9. Cytotoxic and phototoxic effects of zinc(II) phthalocyanine **(7)** against HeLa.

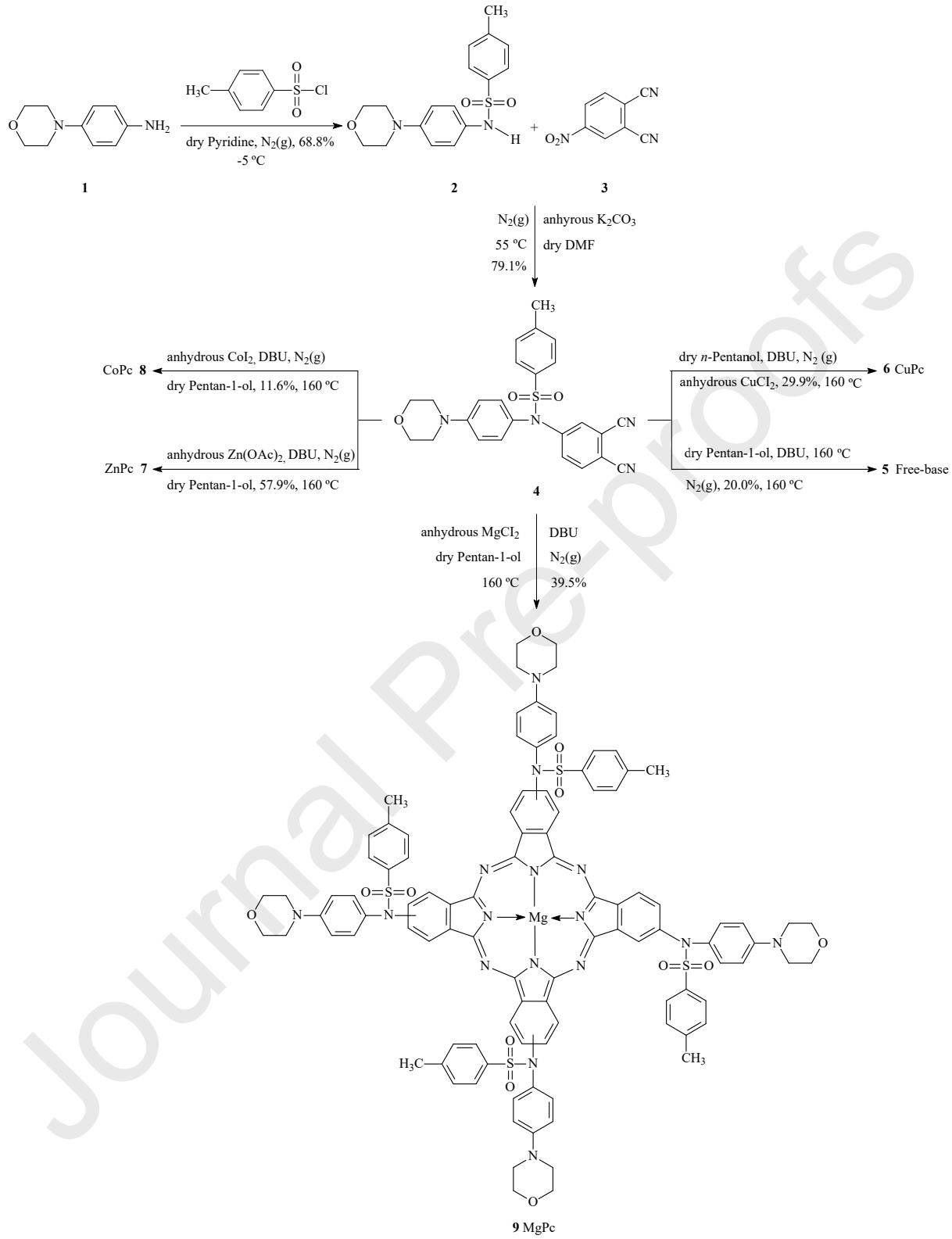

Scheme. The synthesis of the peripheral tetra-substituted free-base **(5)**, copper(II) **(6)**, zinc(II) **(7)**, cobalt(II) **(8)** and magnesium(II) **(9)** phthalocyanine derivatives.

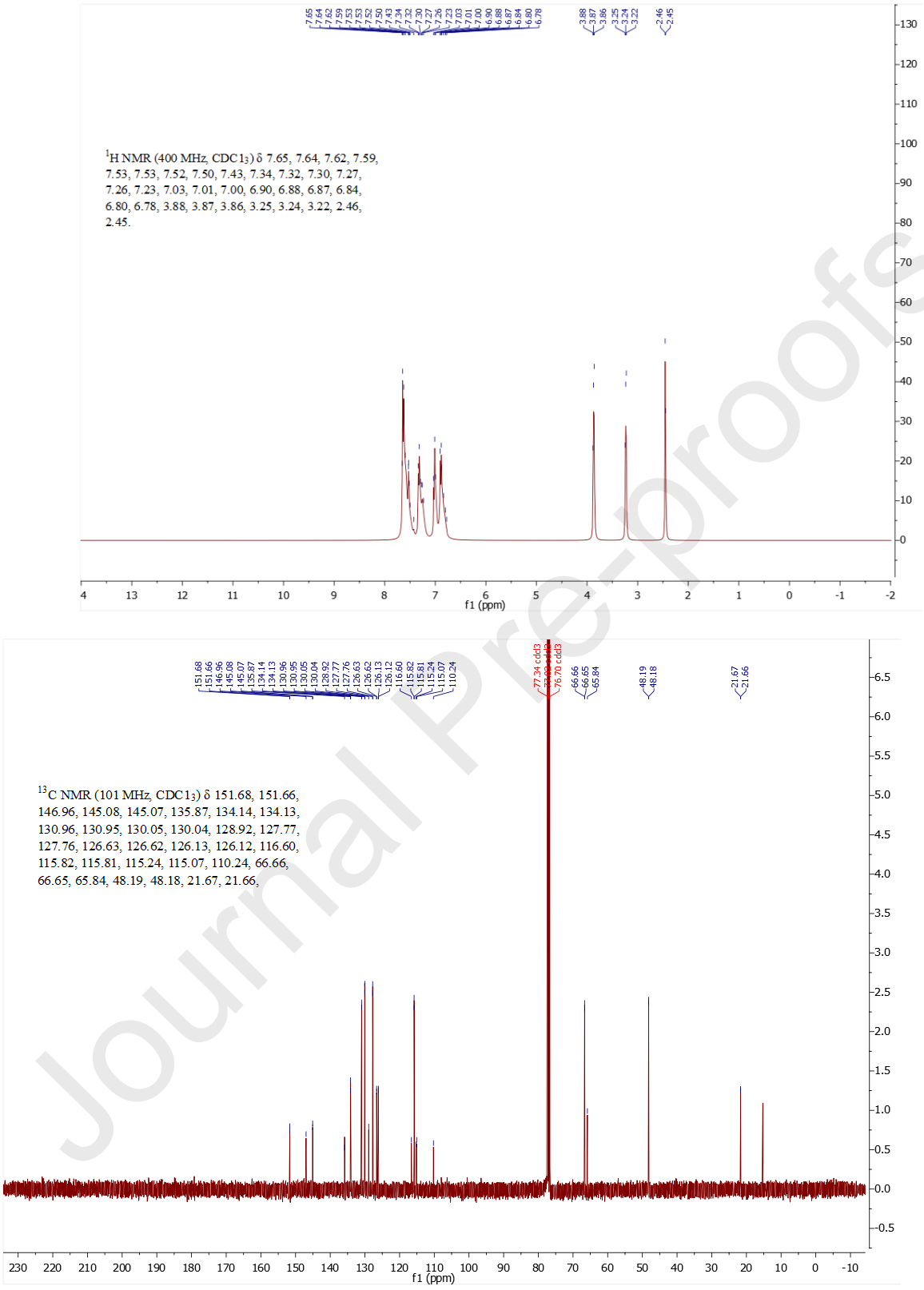

Figure 1. ^{1}H and ^{13}C NMR spectra of the precursor dicyano compound **(4)** in $CDCI_3$.

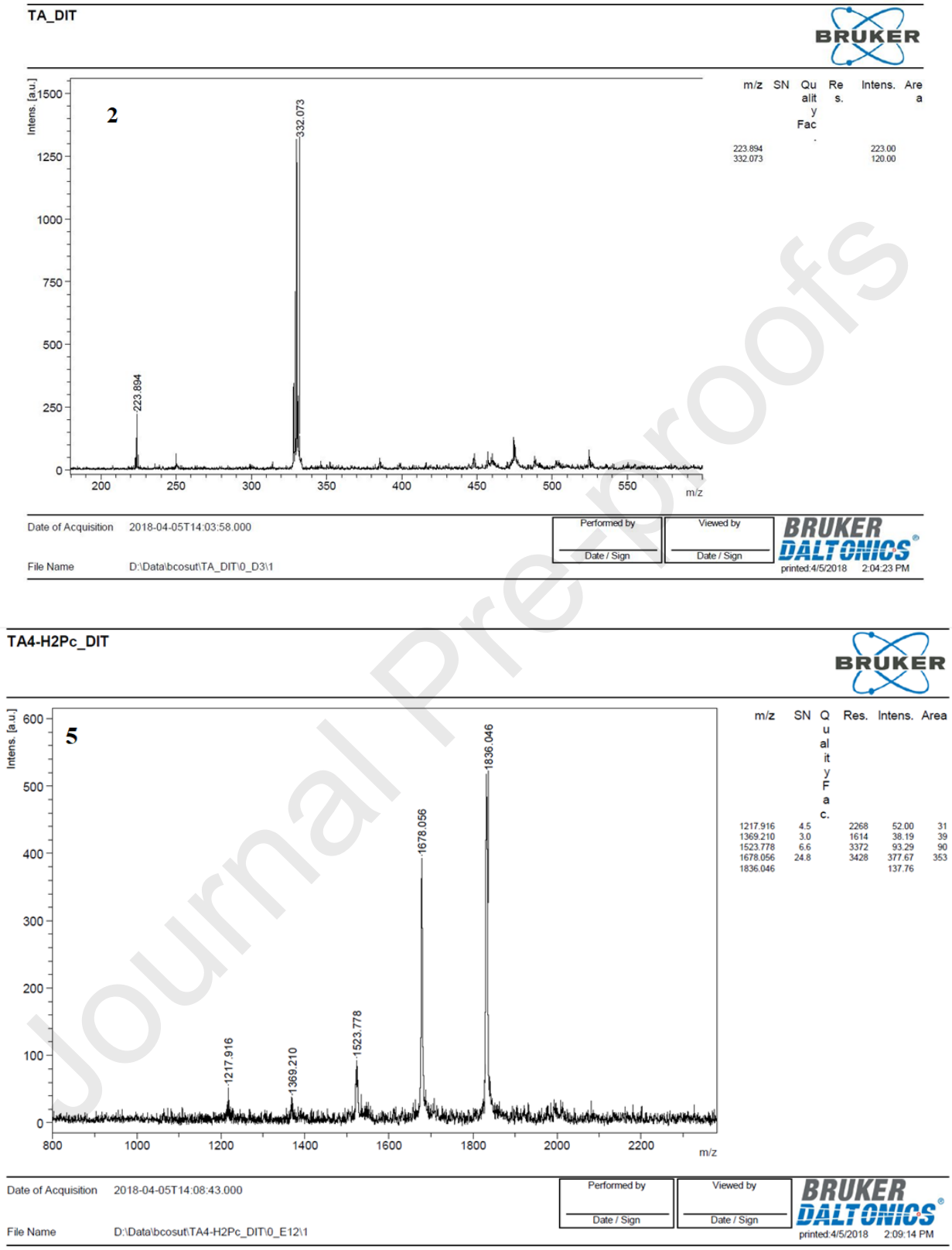

Figure 2. Mass spectral data of the compounds **(2)** and **(5)**.

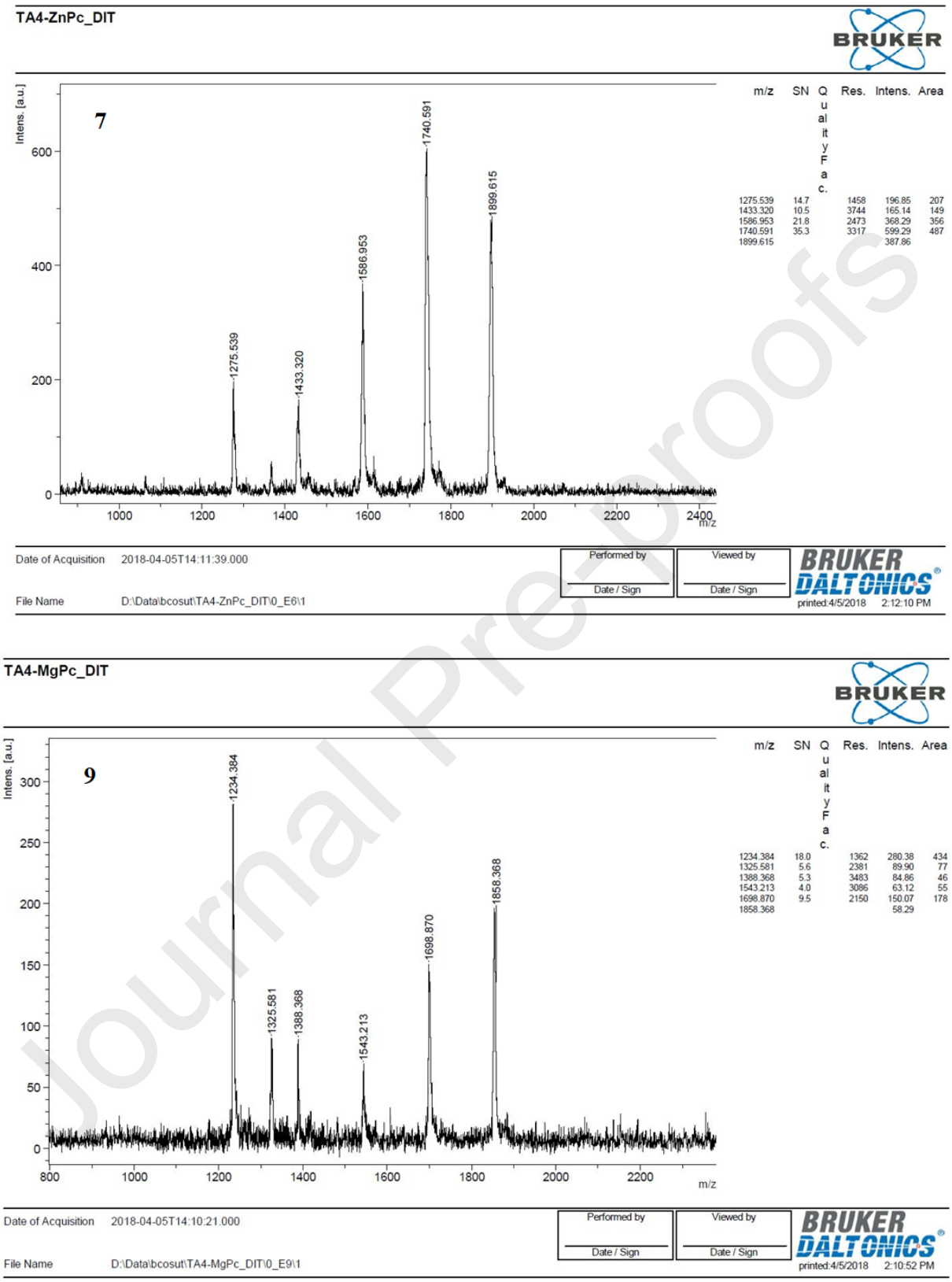

Figure 3. Mass spectral data of the compounds **(7)** and **(9)**.

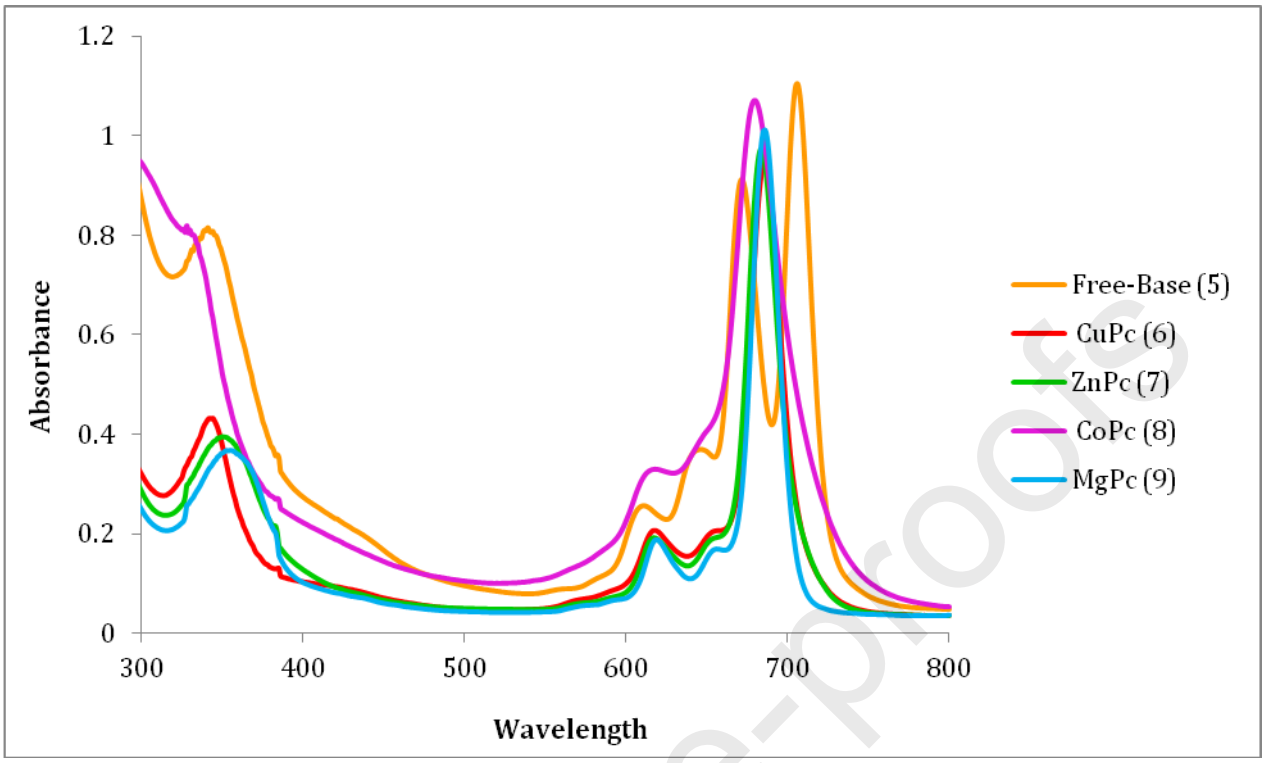

Figure 4. The ground state electronic absorption spectra of new free-base **(5)** copper(II) **(6)**, zinc(II) **(7)**, cobalt(II) **(8)** and magnesium(II) **(9)** phthalocyanines (C = 1.0×10^{-5} M) in chloroform.

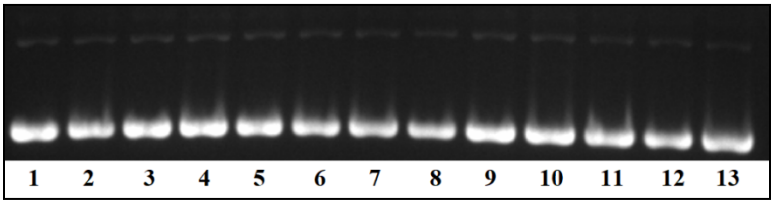

Figure 5. Agarose gel electrophoresis of pBR322 plasmid DNA in the absence and presence of compounds without irradiation. Lane 1, DNA control; lane 2–4, **(6)** (25, 50 and 100 μM); lane 5–7, **(7)** (25, 50 and 100 μM); lane 8–10, **(8)** (25, 50 and 100 μM); lane 11–13, **(9)** (25, 50 and 100 μM).

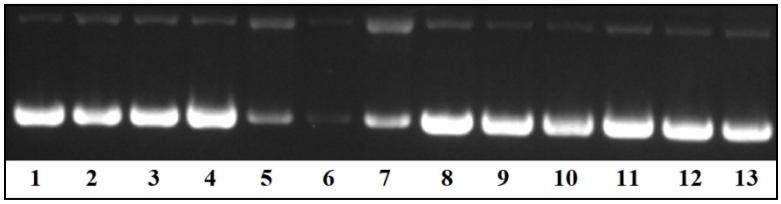

Figure 6. Agarose gel electrophoresis of pBR322 plasmid DNA in the absence and presence of compounds with irradiation (white, 17.5 mW/cm^2, 30 min). Lane 1, DNA control; lane 2–4, **(6)** (25, 50 and 100 μM); lane 5–7, **(7)** (25, 50 and 100 μM); lane 8–10, **(8)** (25, 50 and 100 μM); lane 11–13, **(9)** (25, 50 and 100 μM).

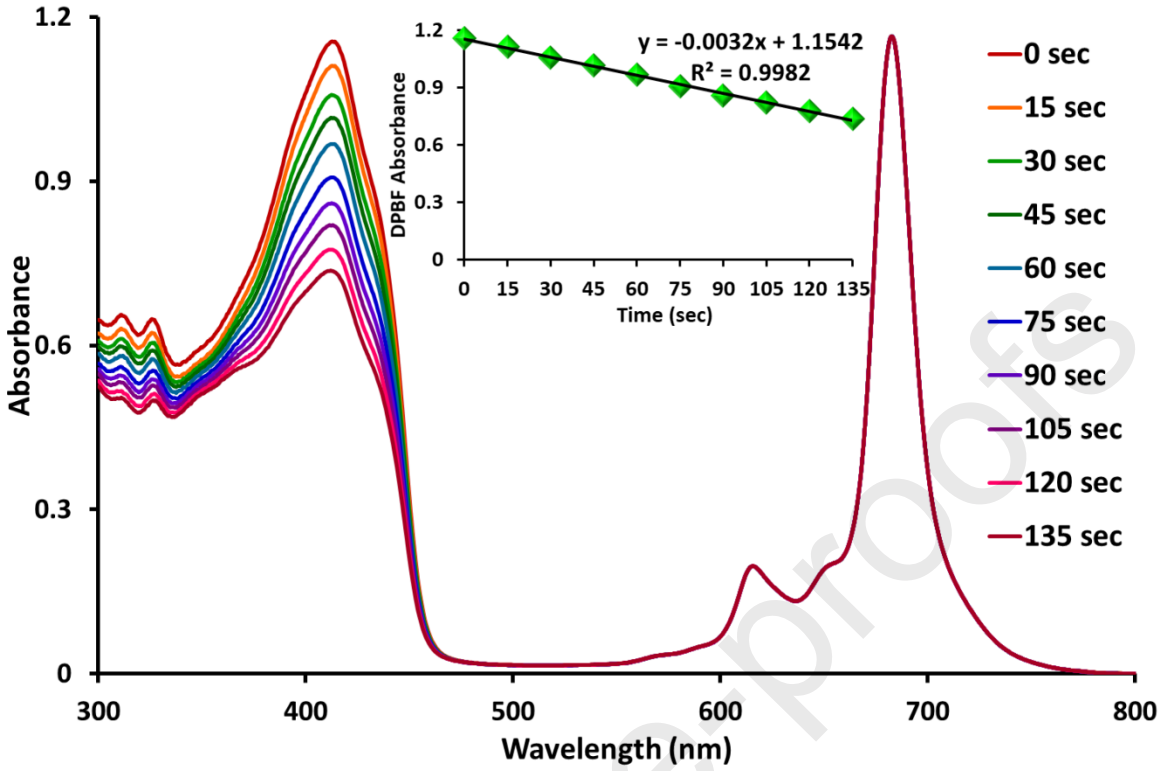

Figure 7. Absorption changes during the determination of singlet oxygen quantum yield for zinc(II) phthalocyanine **(7)** in DMF using DPBF as a singlet oxygen quencher.

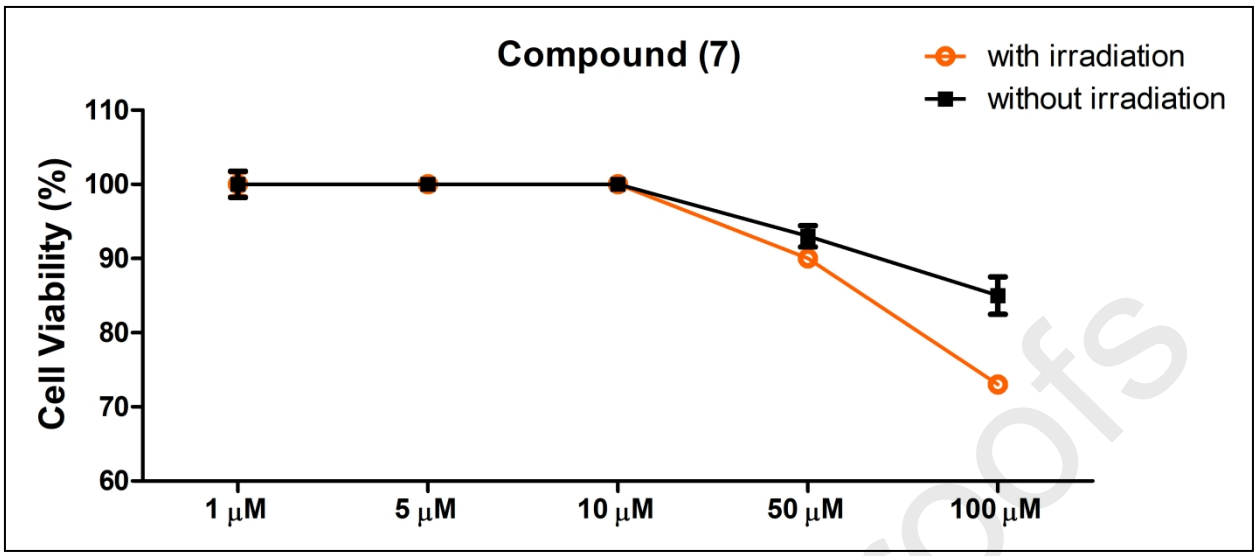

Figure 8. Cytotoxic and phototoxic effects of zinc(II) phthalocyanine **(7)** against HCT-116.

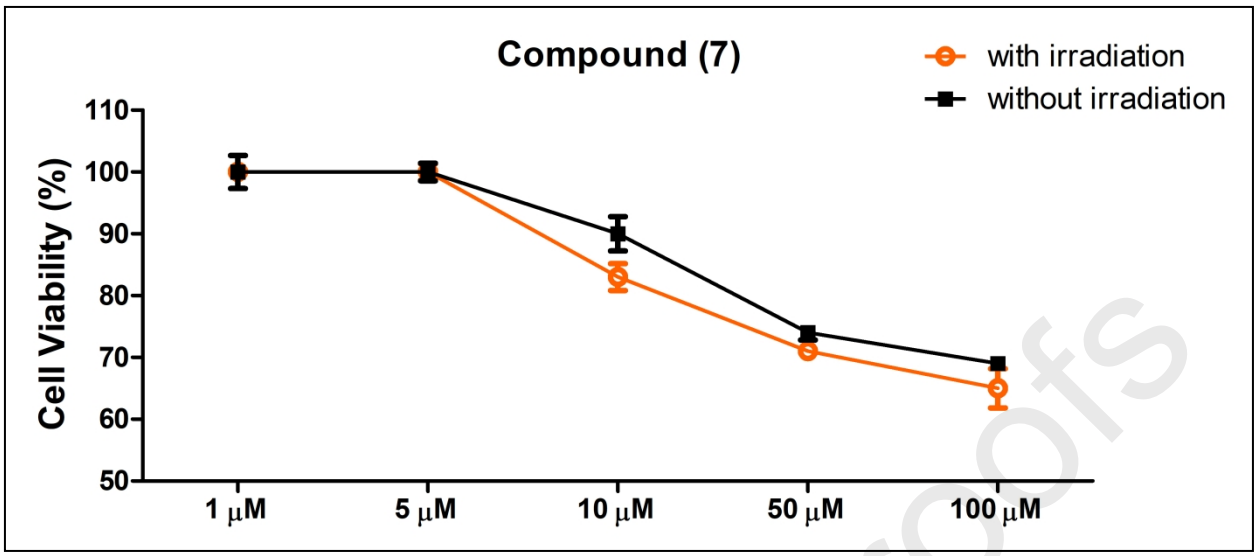

Figure 9. Cytotoxic and phototoxic effects of zinc(II) phthalocyanine **(7)** against HeLa.

Author Contribution Statement for

DNA interaction and anticancer properties of new peripheral phthalocyanines carrying tosylated 4-morpholinoaniline units

Halise Yalazan: Designing, Methodology, Synthesis, Characterization, and Purification.

Burak Barut: DNA cleavage studies, DNA binding studies, Cytotoxicity, and phototoxicity studies.

Beytullah Ertem*: Designing, Methodology, Synthesis, Characterization, Writing-Reviewing, Editing and Visualization.

Can Özgür Yalçın: DNA cleavage studies, DNA binding studies, Cytotoxicity, and phototoxicity studies.

Yasemin Ünver: Designing, Methodology, Synthesis, and Characterization.

Arzu Özel: DNA cleavage studies, DNA binding studies, Cytotoxicity, and phototoxicity studies.

İpek Ömeroğlu: Photochemical studies.

Mahmut Durmuş: Photochemical studies.

Halit Kantekin: Designing, Methodology, Synthesis, Characterization, Purification, Reviewing, Editing and Validation.

Declaration of interests

☒ The authors declare that they have no known competing financial interests or personal relationships that could have appeared to influence the work reported in this paper.

☐The authors declare the following financial interests/personal relationships which may be considered as potential competing interests:

Highlights

1. Morpholine-based new free-base, $Co^{II}Pc$, $Cu^{II}Pc$, $Zn^{II}Pc$, and $Mg^{II}Pc$ were synthesized.

2. New phthalocyanines were verified by common spectroscopic techniques.

3. The photochemical parameters of $Zn^{II}Pc$ **(7)** were examined.

4. DNA cleavage features of $Zn^{II}Pc$ **(7)** were investigated.

5. Cyto/phototoxic features of $Zn^{II}Pc$ **(7)** against cancer cells were examined.